

Figure S1. 6 out of 57 NT trajectories. To facilitate the visualization, the x-y projection of each trajectory is also shown (grey). The position unit on each axis is μm . The time resolution is 32 ms.

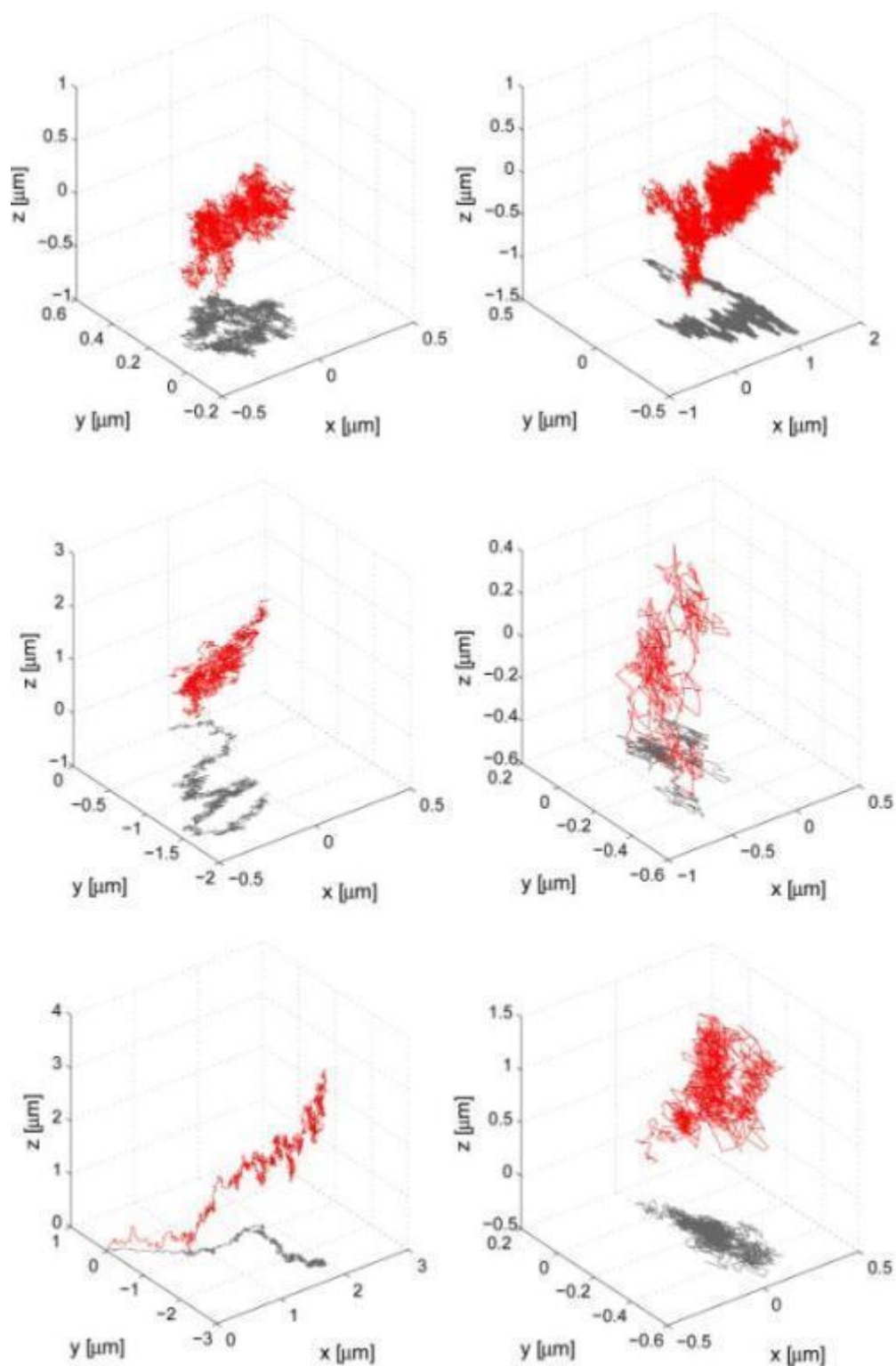


Figure S2. 6 out of 57 NT trajectories. To facilitate the visualization, the x-y projection of each trajectory is also shown (grey). The position unit on each axis is μm . The time resolution is 32 ms.

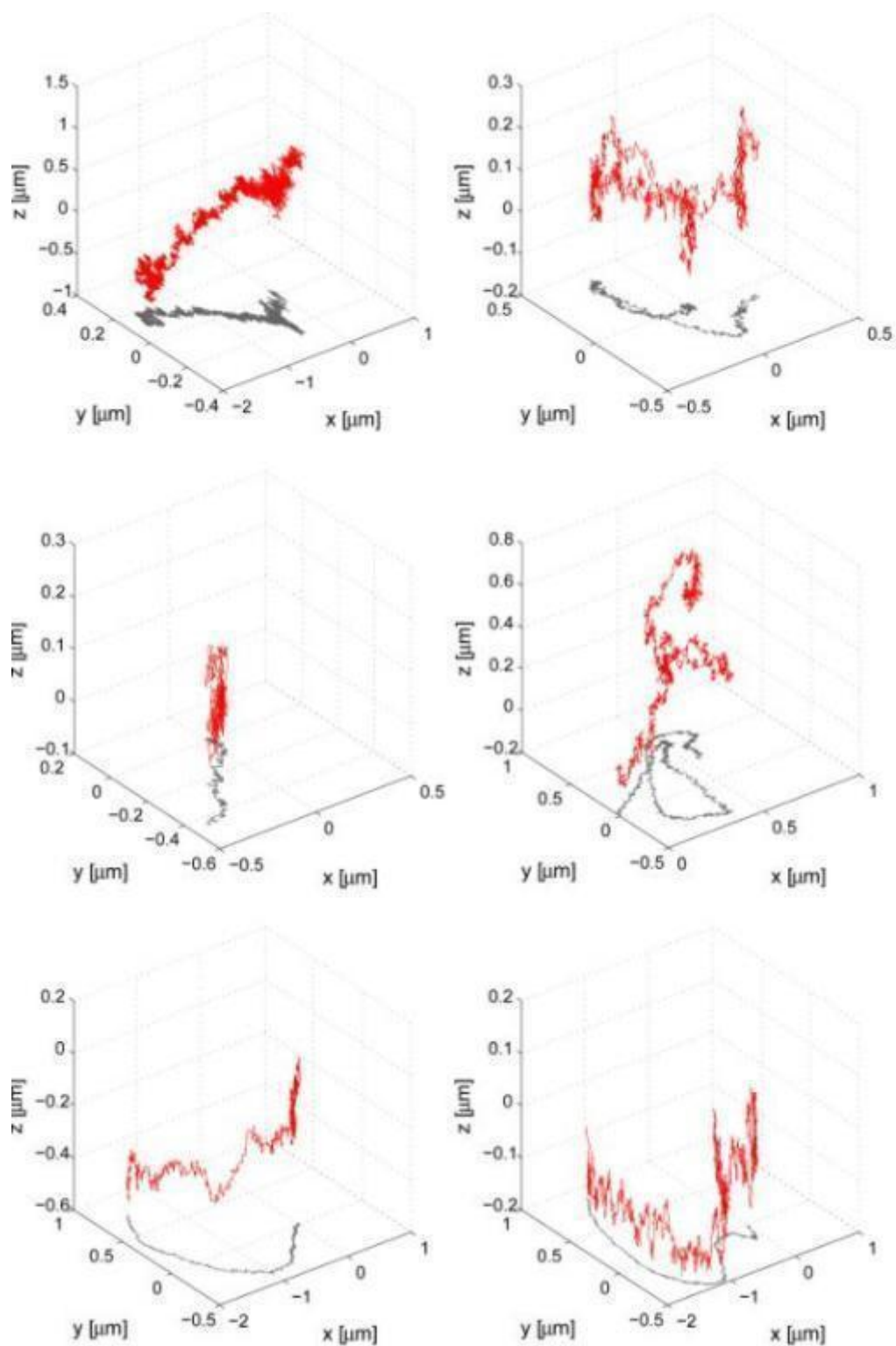


Figure S3. 6 out of 57 NT trajectories. To facilitate the visualization, the x-y projection of each trajectory is also shown (grey). The position unit on each axis is μm . The time resolution is 32 ms.

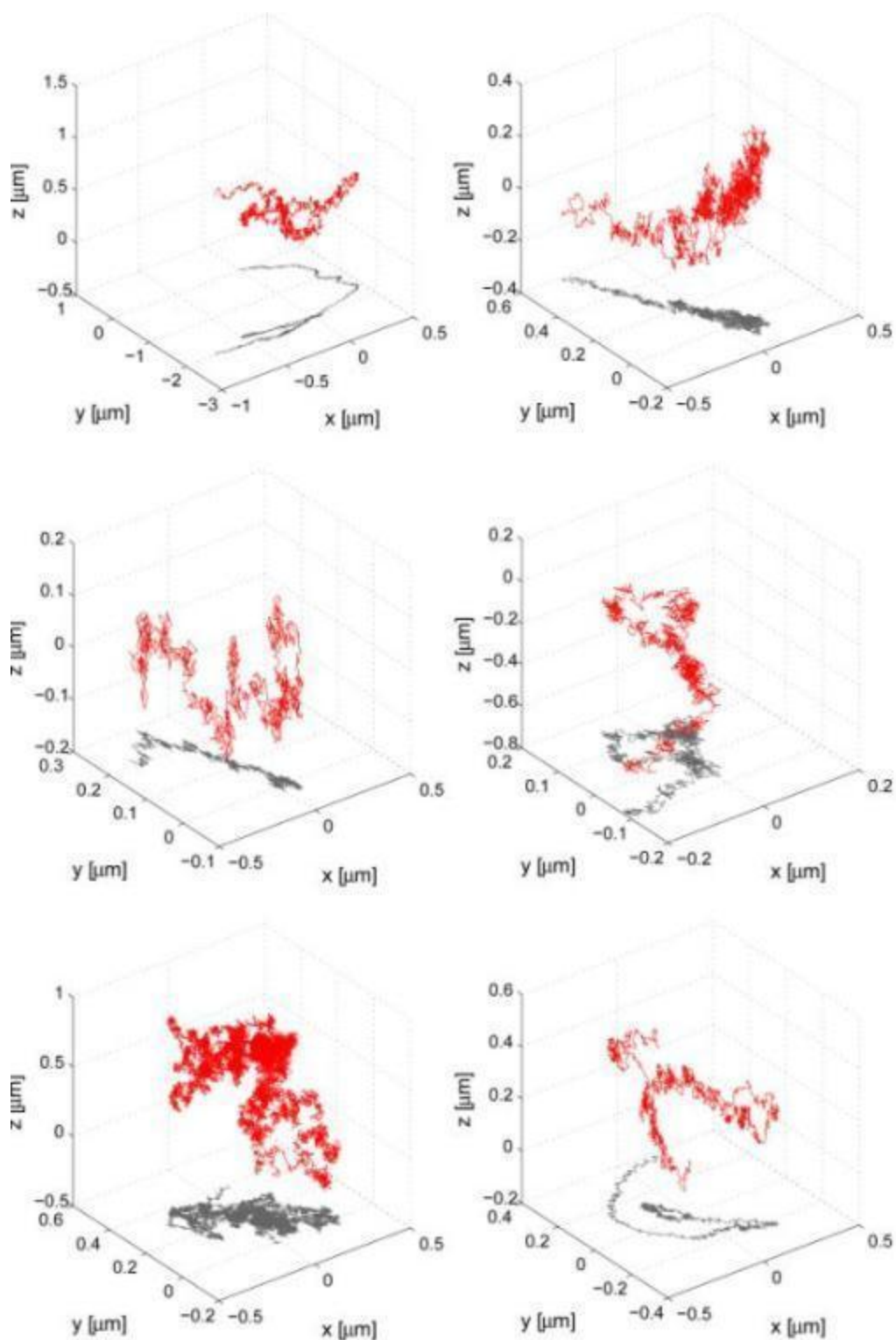


Figure S4. 6 out of 57 NT trajectories. To facilitate the visualization, the x-y projection of each trajectory is also shown (grey). The position unit on each axis is μm . The time resolution is 32 ms.

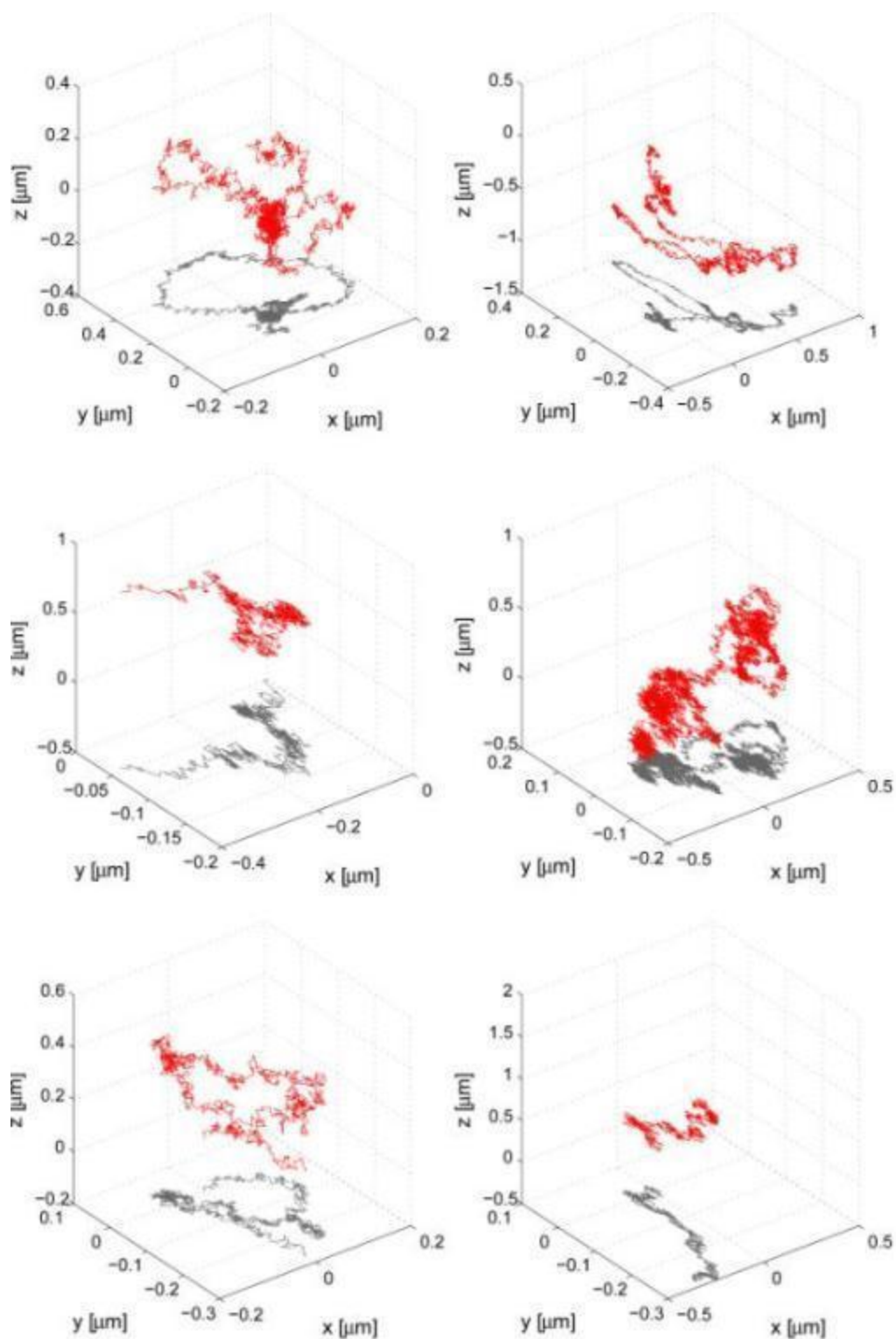


Figure S5. 6 out of 57 NT trajectories. To facilitate the visualization, the x-y projection of each trajectory is also shown (grey). The position unit on each axis is μm . The time resolution is 32 ms.

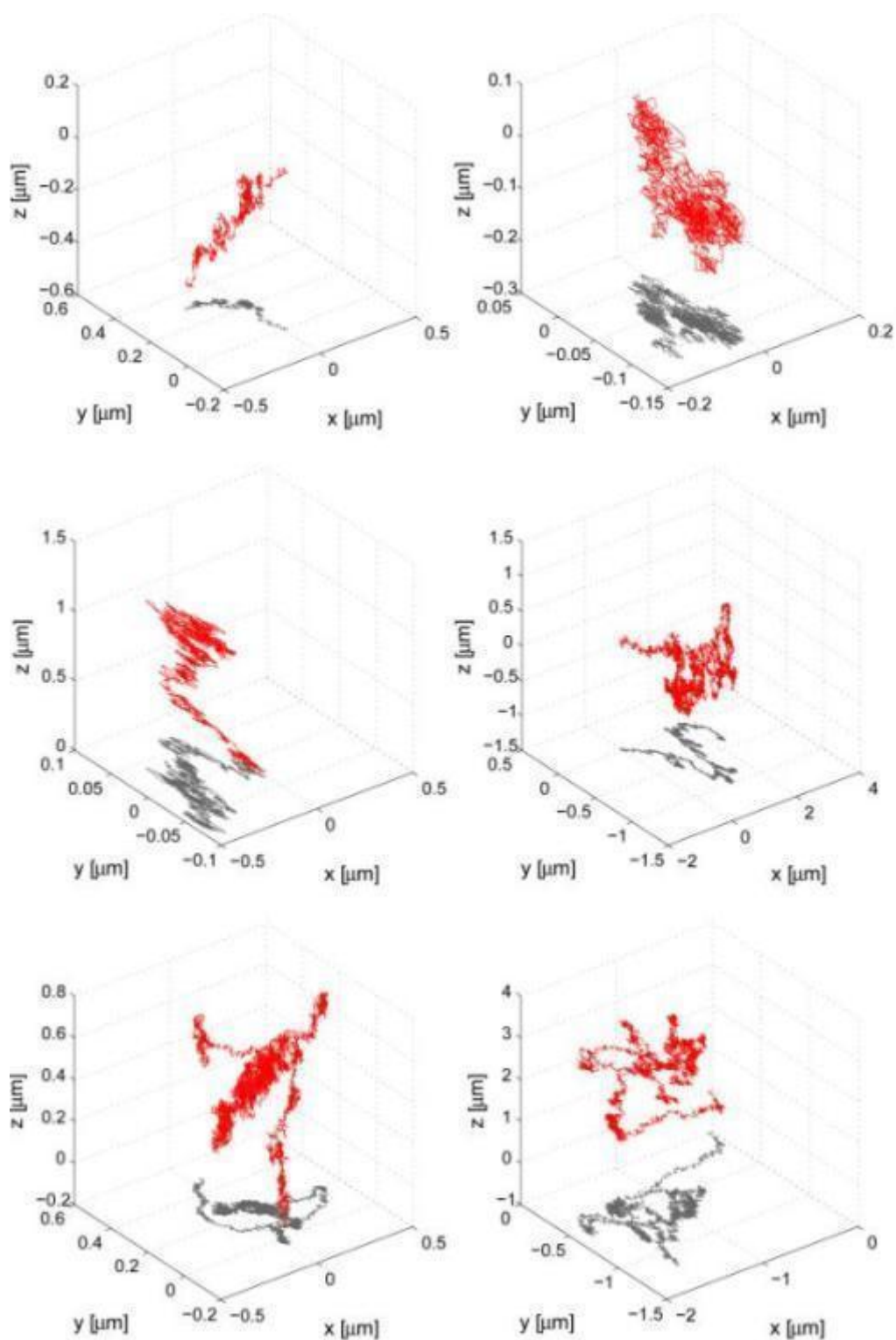


Figure S6. 6 out of 57 NT trajectories. To facilitate the visualization, the x-y projection of each trajectory is also shown (grey). The position unit on each axis is μm . The time resolution is 32 ms.

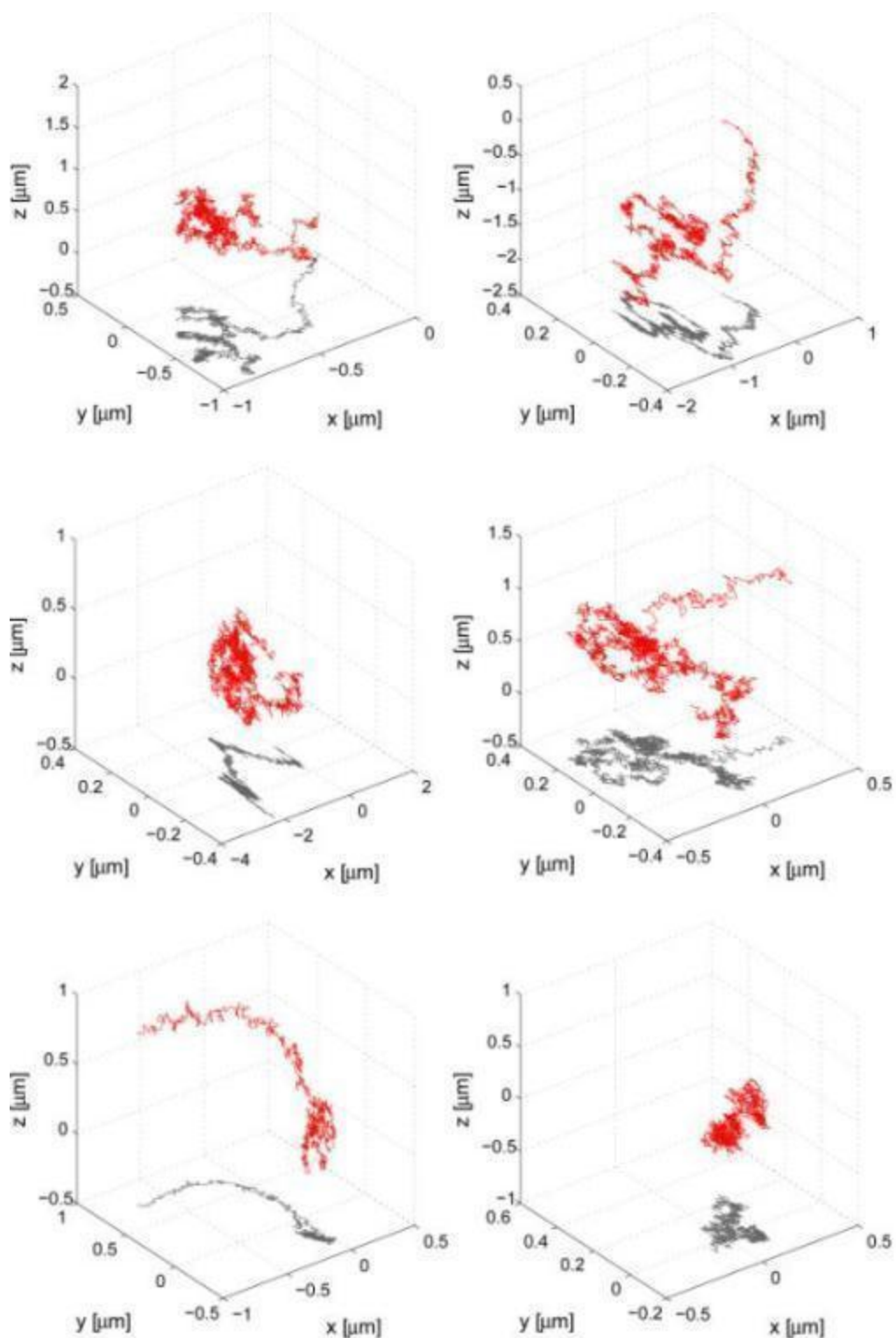


Figure S7. 6 out of 57 NT trajectories. To facilitate the visualization, the x-y projection of each trajectory is also shown (grey). The position unit on each axis is μm . The time resolution is 32 ms.

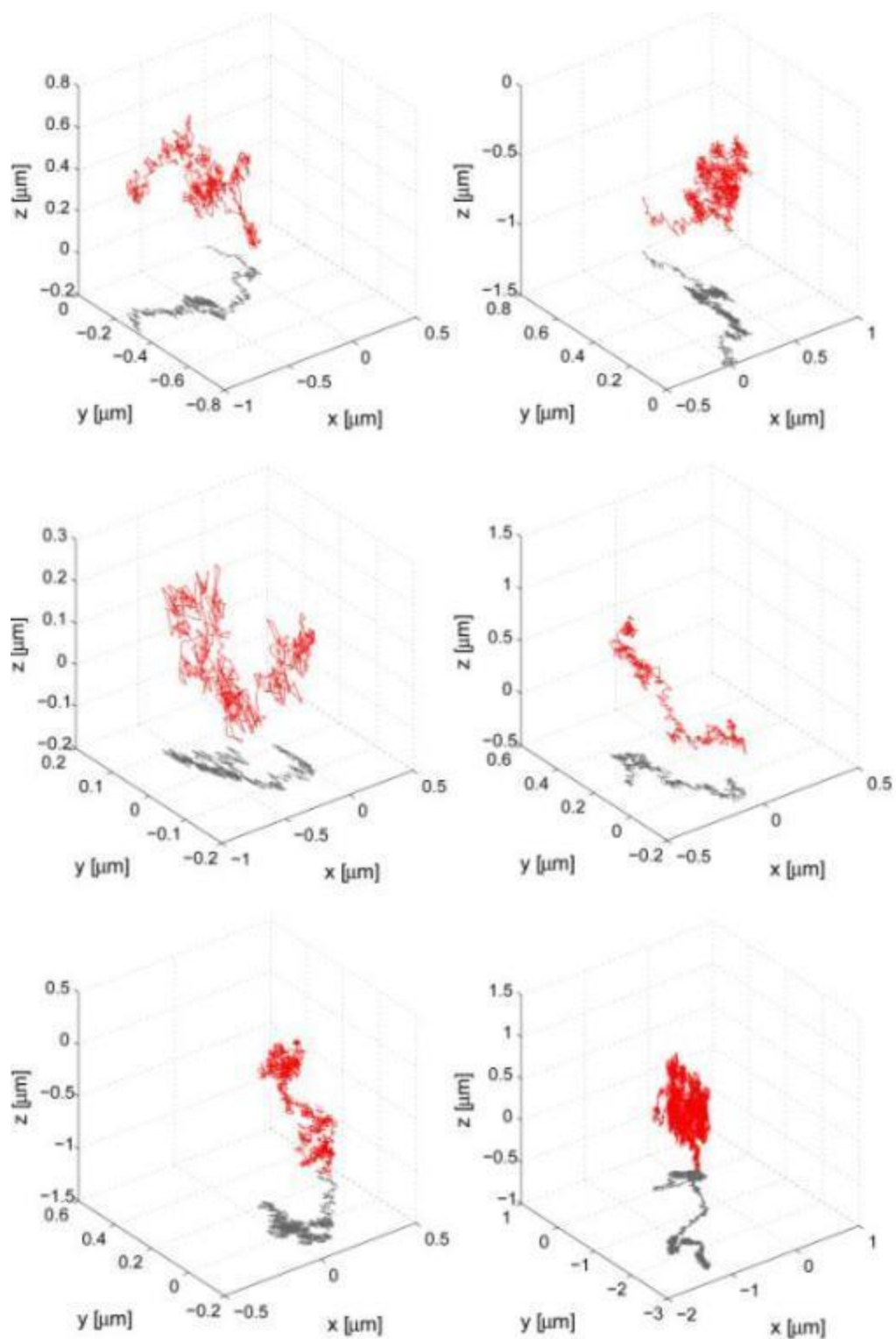


Figure S8. 6 out of 57 NT trajectories. To facilitate the visualization, the x-y projection of each trajectory is also shown (grey). The position unit on each axis is μm . The time resolution is 32 ms.

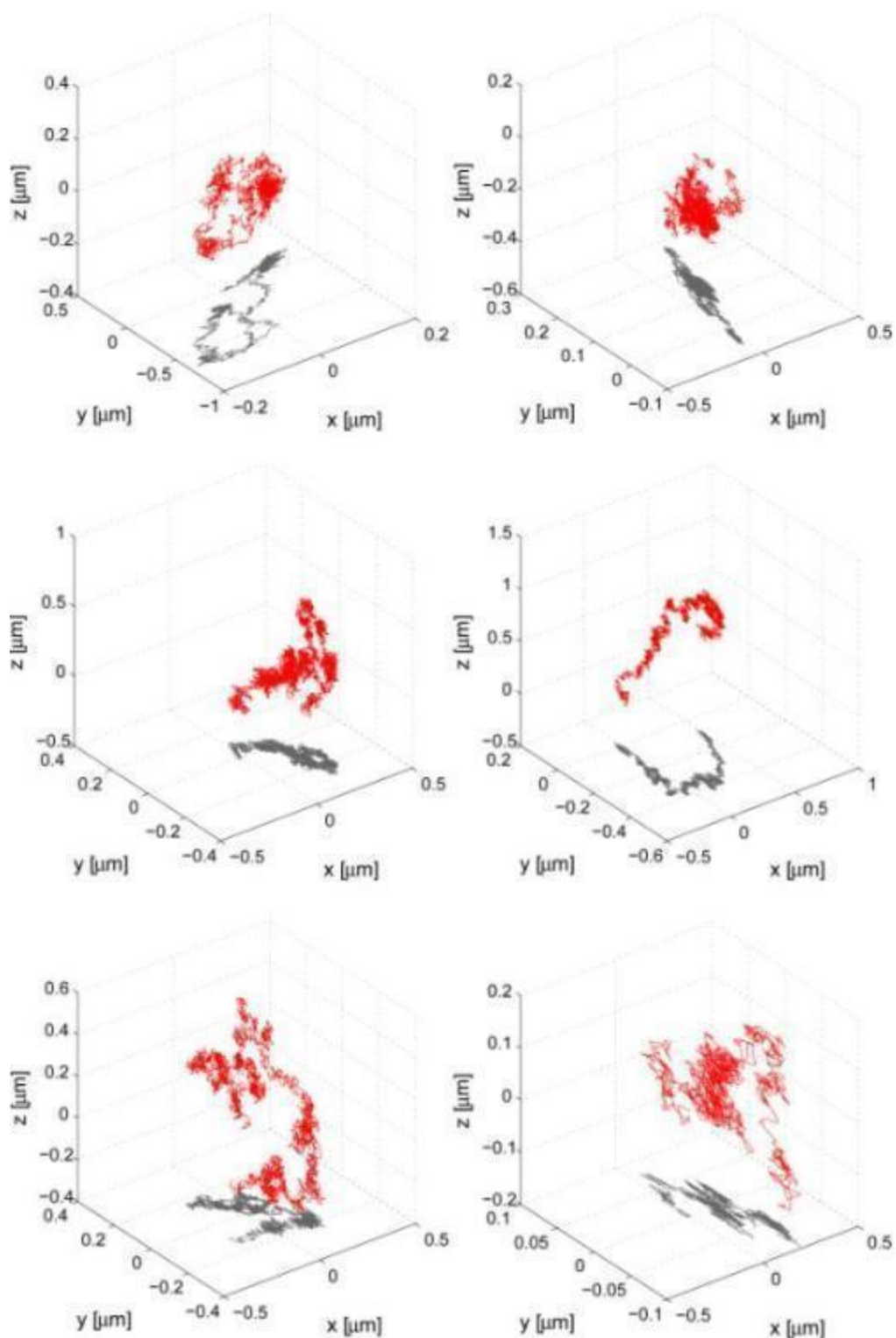


Figure S9. 6 out of 57 NT trajectories. To facilitate the visualization, the x-y projection of each trajectory is also shown (grey). The position unit on each axis is μm . The time resolution is 32 ms.

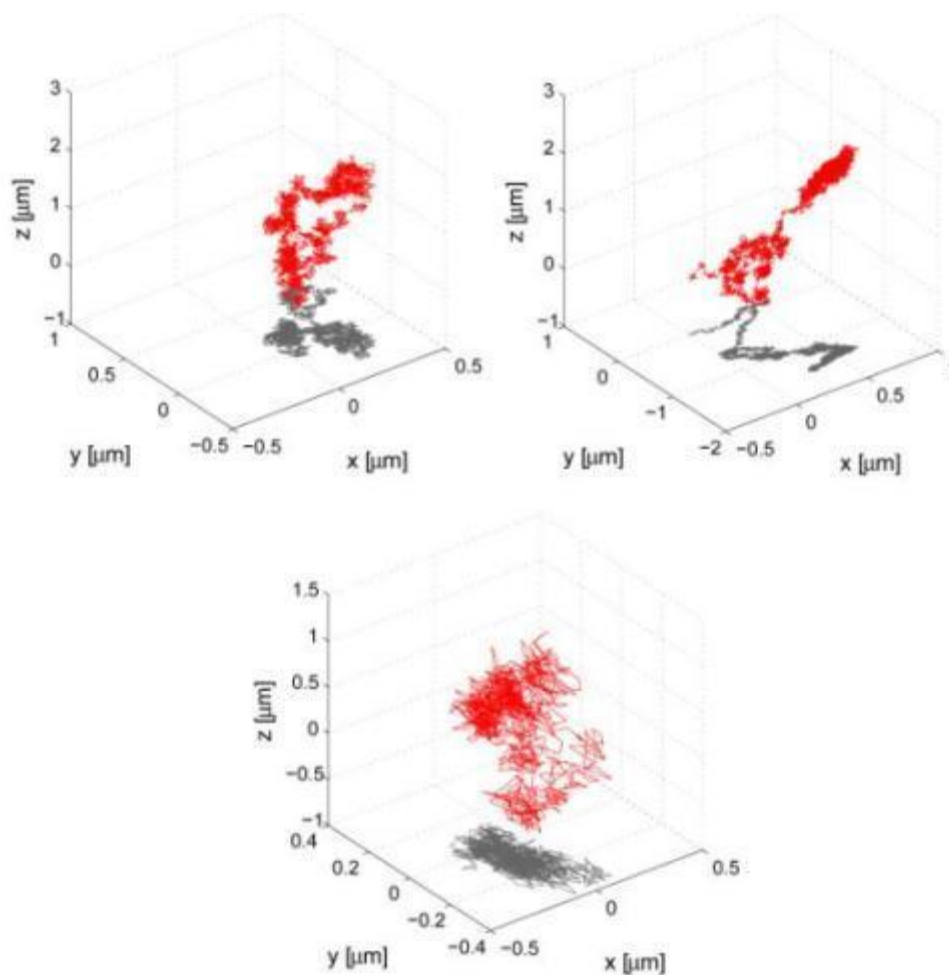


Figure S10. 3 out of 57 NT trajectories. To facilitate the visualization, the x-y projection of each trajectory is also shown (grey). The position unit on each axis is μm . The time resolution is 32 ms.

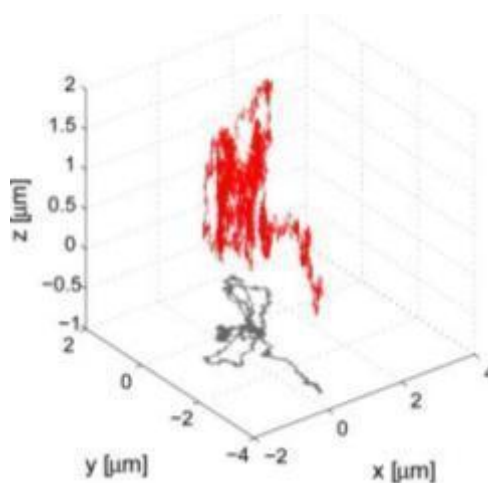


Figure S11. 1 out of 25 LAT trajectories. To facilitate the visualization, the x-y projection of each trajectory is also shown (grey). The position unit on each axis is μm . The time resolution is 32 ms.

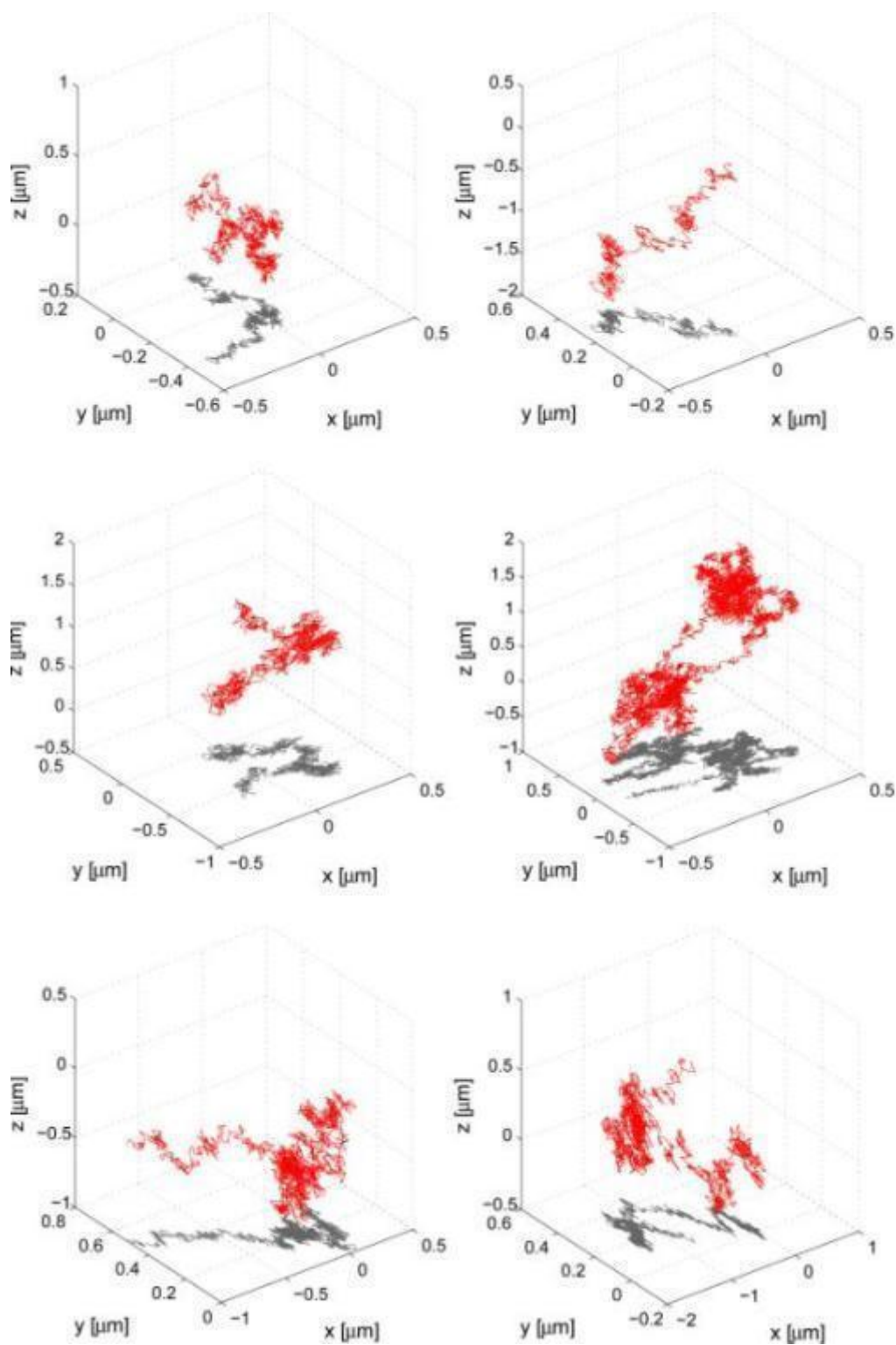


Figure S12. 6 out of 25 LAT trajectories. To facilitate the visualization, the x-y projection of each trajectory is also shown (grey). The position unit on each axis is μm . The time resolution is 32 ms.

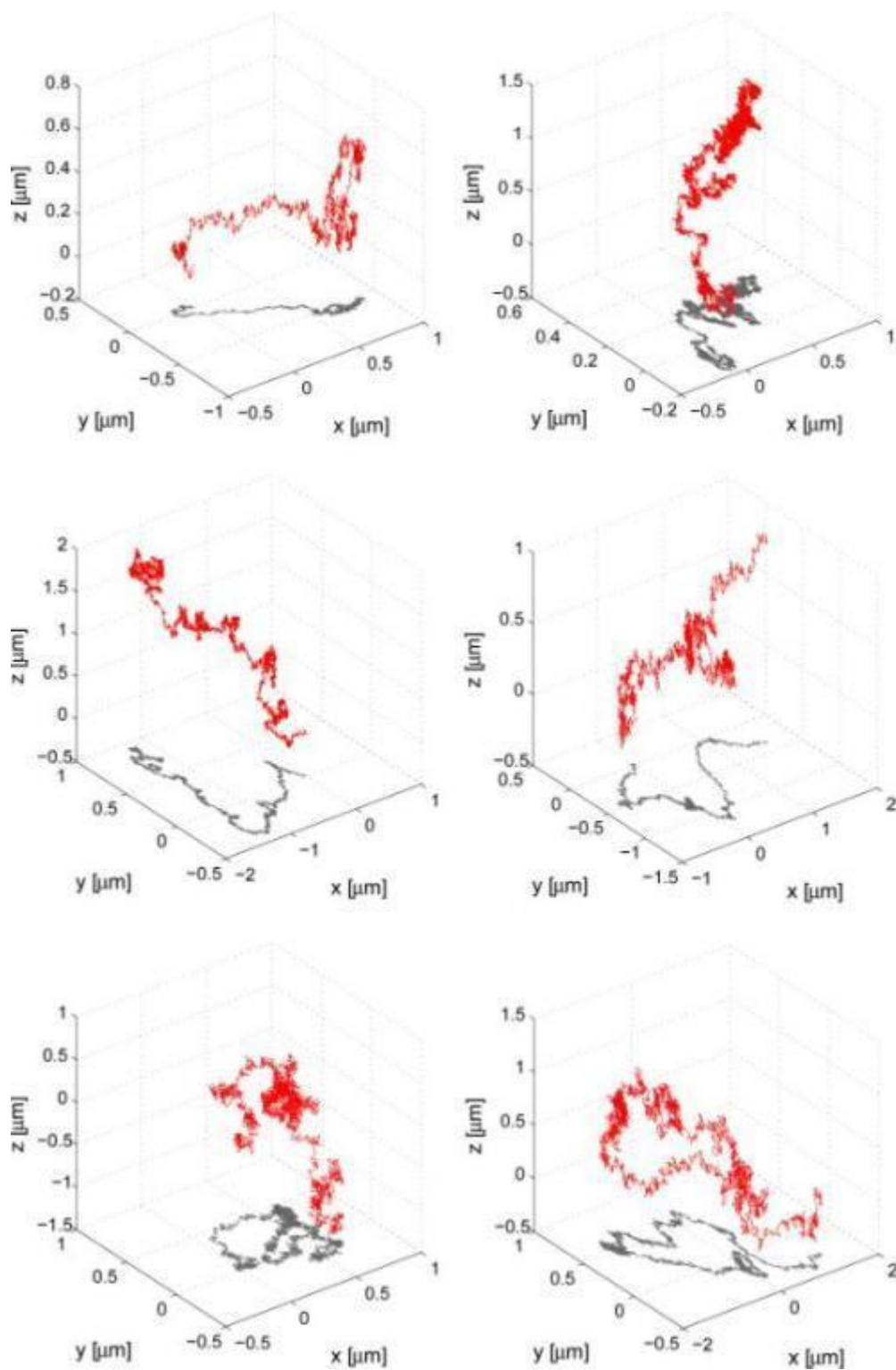


Figure S13. 6 out of 25 LAT trajectories. To facilitate the visualization, the x - y projection of each trajectory is also shown (grey). The position unit on each axis is μm . The time resolution is 32 ms.

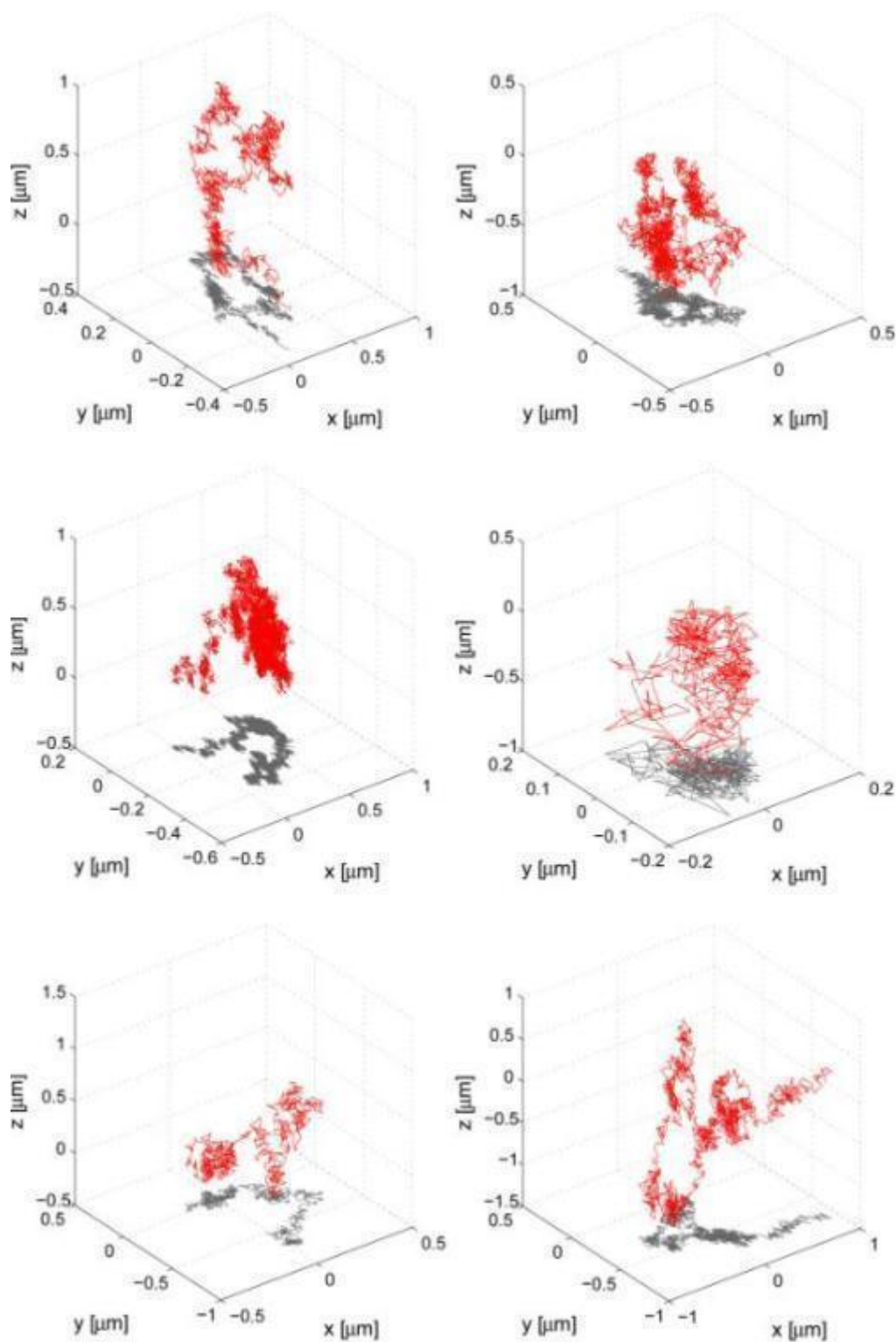


Figure S14. 6 out of 25 LAT trajectories. To facilitate the visualization, the x-y projection of each trajectory is also shown (grey). The position unit on each axis is μm . The time resolution is 32 ms.

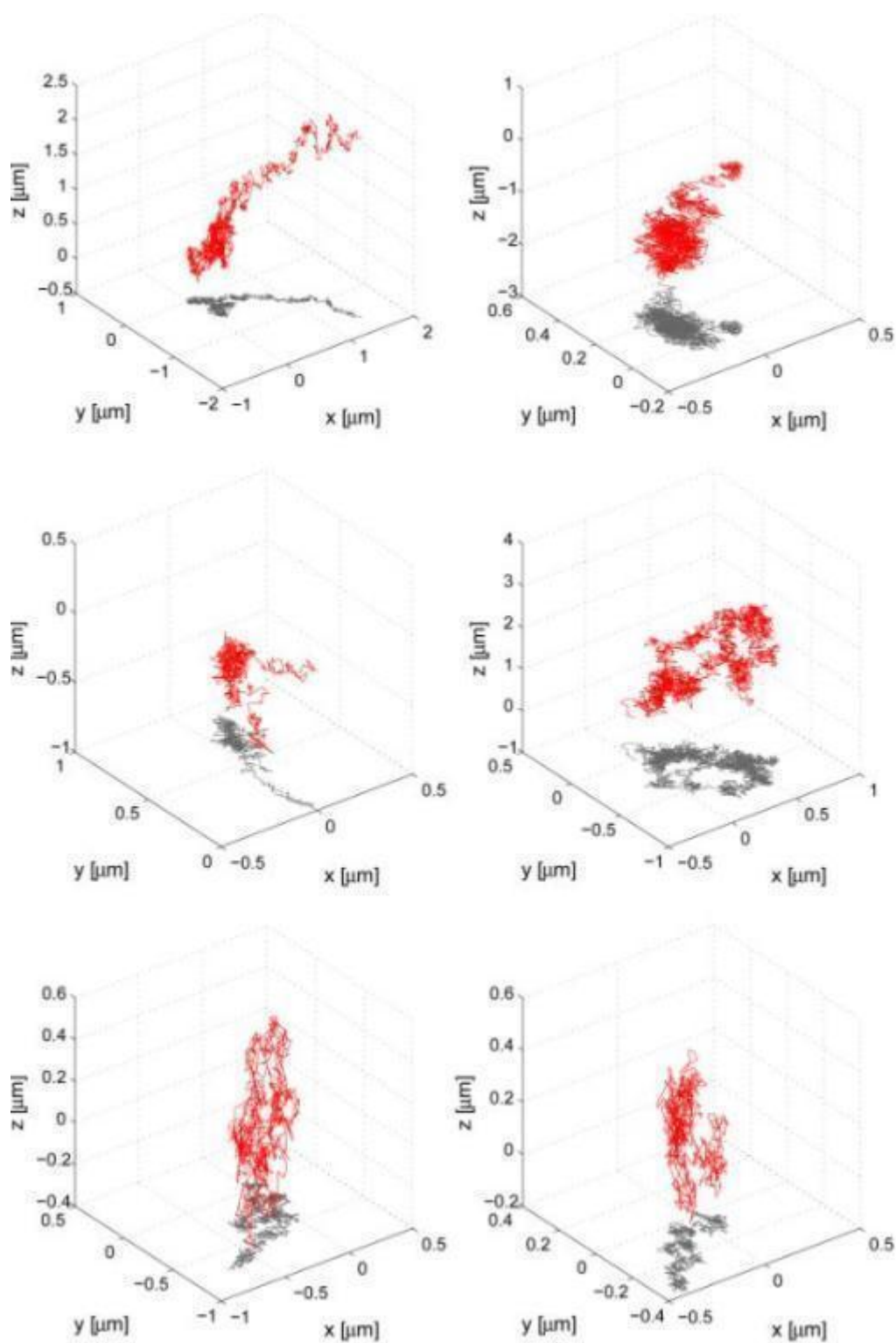


Figure S15. 6 out of 25 LAT trajectories. To facilitate the visualization, the x-y projection of each trajectory is also shown (grey). The position unit on each axis is μm . The time resolution is 32 ms.

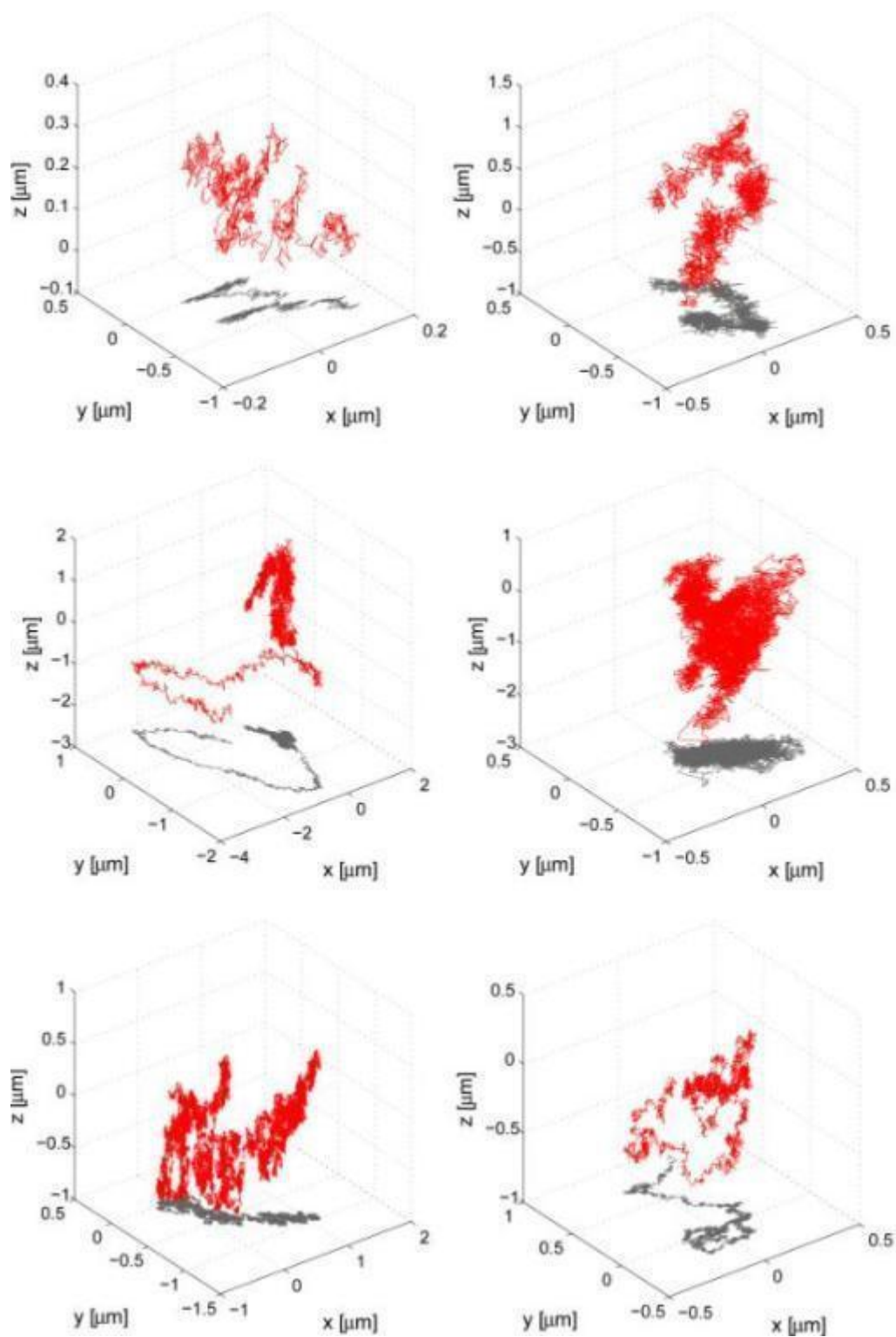


Figure S16. 6 out of 20 NCZ trajectories. To facilitate the visualization, the x-y projection of each trajectory is also shown (grey). The position unit on each axis is μm . The time resolution is 32 ms.

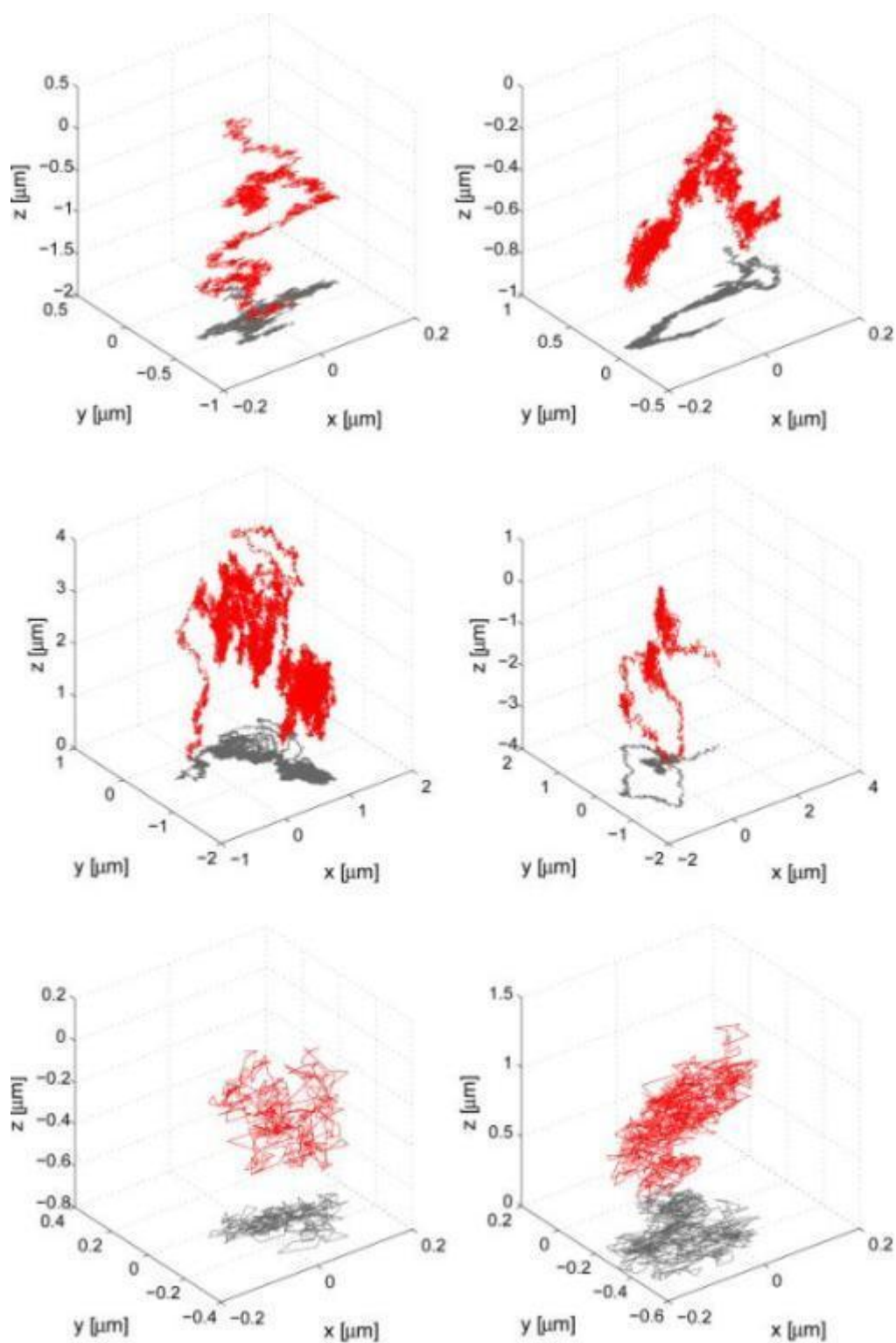


Figure S17. 6 out of 20 NCZ trajectories. To facilitate the visualization, the x-y projection of each trajectory is also shown (grey). The position unit on each axis is μm . The time resolution is 32 ms.

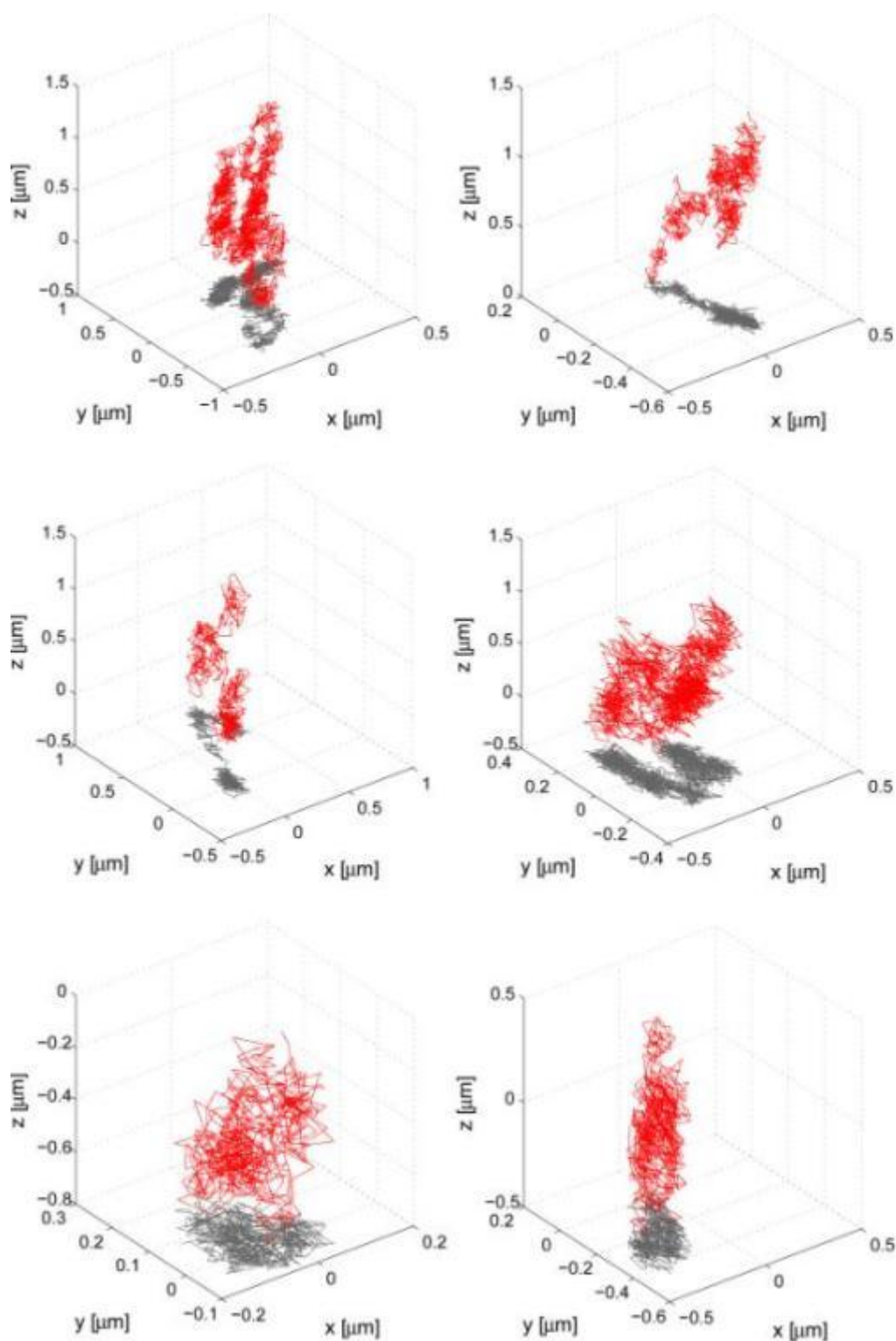


Figure S18. 6 out of 20 NCZ trajectories. To facilitate the visualization, the x-y projection of each trajectory is also shown (grey). The position unit on each axis is μm . The time resolution is 32 ms.

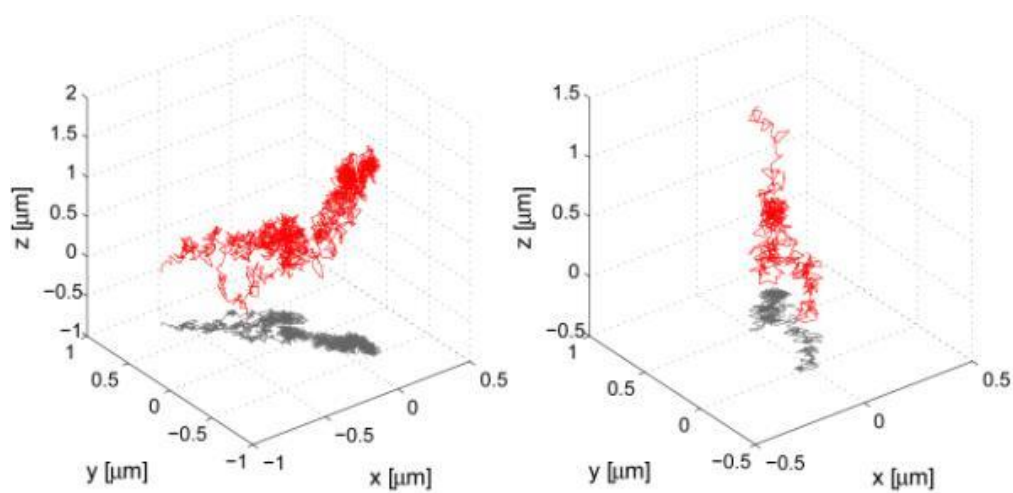


Figure S19. 2 out of 20 NCZ trajectories. To facilitate the visualization, the x-y projection of each trajectory is also shown (grey). The position unit on each axis is μm . The time resolution is 32 ms.

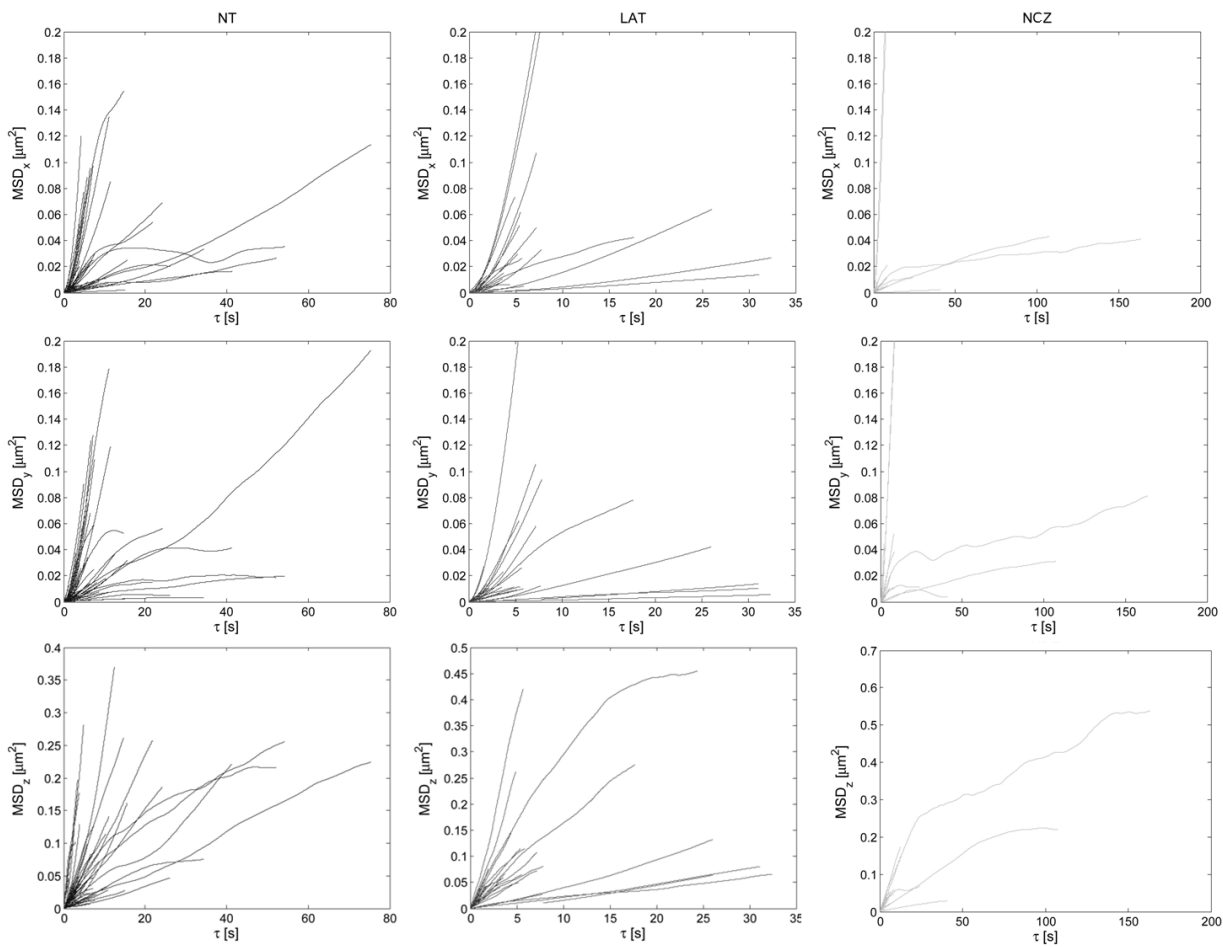


Figure S20. All 102 MSD curves: plots in columns and rows match the categories (NT, LAT and NCZ) and the one-dimensional direction of the calculated MSD (MSD_x , MSD_y and MSD_z).

Division by type

The algorithm we used is based on a comparison between the finite integral of the experimental MSD and the finite integral of the Brownian MSD (i.e. the line connecting the point (0;0) and the calculated MSD at $\tau = m\delta t$). Given a control percentage c and

$$\Delta = \int_0^{m\delta t} MSD_{\alpha}(n\delta t)dn - \int_0^{m\delta t} \frac{MSD_{\alpha}(m\delta t)}{m\delta t} n dn \quad (1)$$

$$\Sigma = \int_0^{m\delta t} MSD_{\alpha}(n\delta t)dn + \int_0^{m\delta t} \frac{MSD_{\alpha}(m\delta t)}{m\delta t} n dn \quad (2)$$

where $m\delta t$ is the maximum lag time (chosen according to the aforementioned criterion, i.e. to keep the statistical uncertainty small), it follows that: i) if $\Delta > 0$ and $|\Delta/\Sigma| > c$ then the MSD curve belongs to the confined type; ii) if $\Delta < 0$ and $|\Delta/\Sigma| > c$ the MSD curve belongs to the directed type; iii) otherwise, it belongs to the Brownian one. The control percentage c is chosen in order to distinguish a directed motion curve with a specific D/v ratio, calculated from the expected values of D and v according to the literature. In addition to compare the percentage of trajectories in each type, it is possible to fit the curves with the appropriate models (eqn (2), eqn (3), eqn (4)) in order to get the physical parameters D_{α} , L_{α} and v_{α} . The distribution of short-term diffusion coefficients is an interesting tool to distinguish and characterize the modes of motion. Saxton¹ found it to be highly dependent on the definition of short-term coefficient considered. A short-term coefficient is defined as the slope of a linear fit of the first MSD points. Varying the number N of total points available and the maximum lag time, the most satisfactory definition (at least in the simulations) was found to be $D(0;4)$, that represents a fitting of the first 5 points.

Gyration Tensor

The gyration tensor provides information on the shape of the trajectory. Considering a 3-dimensional space, the trajectory is a set of 3 position vectors of lengths equal to N . The elements of T are given by:

$$T_{ii} = \frac{1}{N} \sum_{k=1}^N (x_{ik} - \langle x_i \rangle) (x_{ik} - \langle x_i \rangle) \quad (3)$$

where x_{ik} is the i -th component (i.e. $x_1 = x$, $x_2 = y$ and $x_3 = z$) of the position vector of the k -th point in the trajectory. The quantity $\langle x_i \rangle$ is the average over the trajectory

$$\langle x_i \rangle = \frac{1}{N} \sum_{i=1}^N x_{i1} \quad (4)$$

The 3 by 3 tensor has as its eigenvalues the principal radii of gyration of the trajectory. Thus, when diagonalised,

$$T = \begin{pmatrix} R_1^2 & 0 & 0 \\ 0 & R_2^2 & 0 \\ 0 & 0 & R_3^2 \end{pmatrix} \quad (5)$$

Rudnick *et al.*² defined a parameter A_3 which measures the asphericity of a trajectory and thereby provides a useful description of deviations from spherical symmetry. A_3 could be expressed in terms of the invariants of the gyration tensor:

$$A_3 = \frac{1}{2} \left[3 \frac{\langle R_1^4 \rangle + \langle R_2^4 \rangle + \langle R_3^4 \rangle}{(\langle R_1^2 + R_2^2 + R_3^2 \rangle)^2} - 1 \right] \quad (6)$$

In the large N limit, it has been calculated for unrestricted random walks:

$$A_3^{RW} = \frac{10}{19} \quad (7)$$

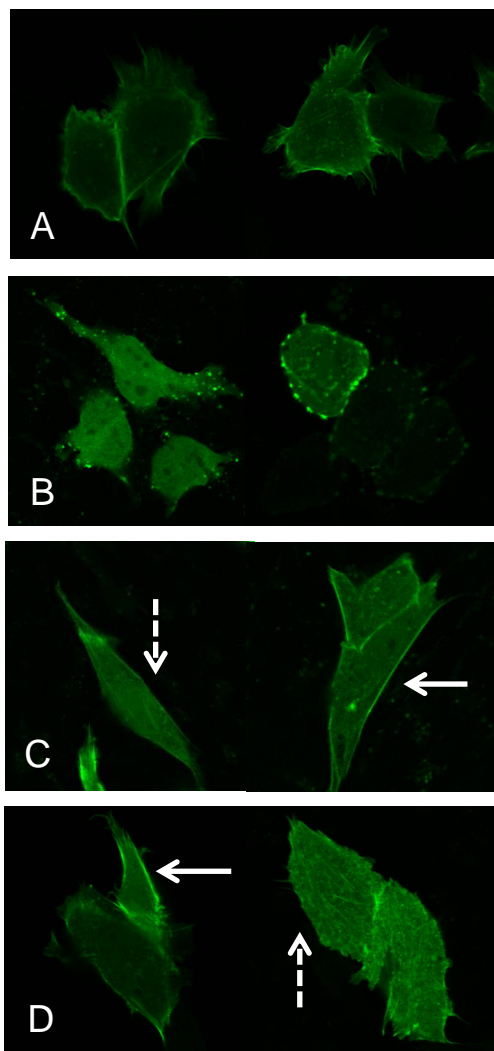


Figure S21. Actin cytoskeleton staining of CHO cells by Actin-Green Fluorescent Protein (panel A). Actin cytoskeleton recovery after Latrunculin B-treatment: $t=0$ (panel B); $t=4h$ (panel C); $t=8h$ (panel D). Solid lines indicate newly formed microfilaments, while dotted lines indicate regions of the plasma membrane where only poorly formed, if any, actin microfilaments are visible.

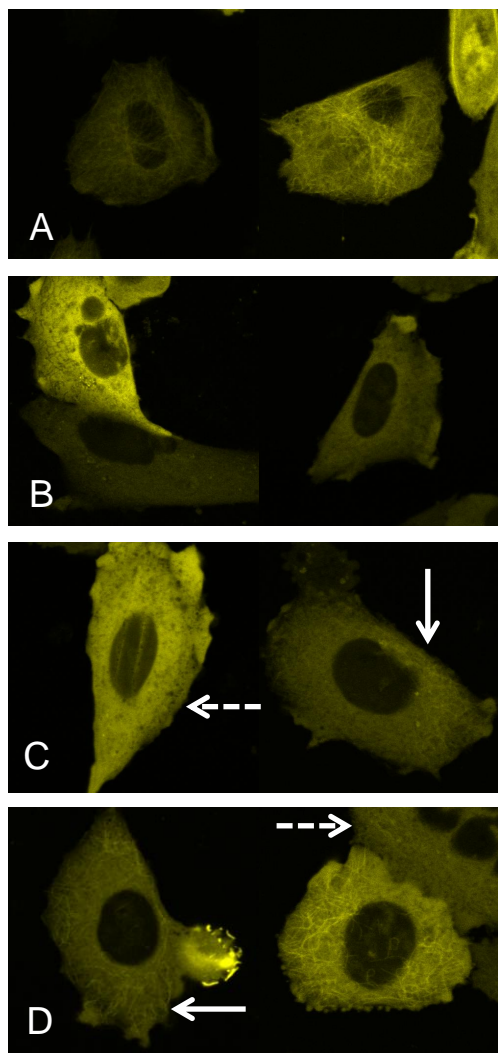


Figure S22. Tubulin cytoskeleton staining of CHO cells by Tubulin-Yellow Fluorescent Protein (panel A). Tubulin cytoskeleton recovery after Nocodazole-treatment: $t=0$ (panel B); $t=4h$ (panel C); $t=8h$ (panel D). Solid lines indicate newly formed microtubules, while dotted lines indicate regions of the plasma membrane where only poorly formed, if any, microtubules can be seen.

Supporting References

1. M.J. Saxton, *Biophys. J.*, 1997, **72**, 1744-1753.
2. J. Rudnick and G. Gaspari, *J. Phys. A-Math. Gen.*, 1986, **19**, L191-L193.